









## Plasma O<sub>2</sub> modifies the structure of synthetic zeolite-A to improve the removal of cadmium ions from aqueous solutions

Alaa FAHMY<sup>1,\*</sup>, Ahmed ELZAREF<sup>1</sup>, Hanan YOUSSEF<sup>2</sup>, Hassan SHEHATA<sup>1</sup>,  
Magdy WASSEL<sup>1</sup>, Jörg FRIEDRICH<sup>3</sup>, Fabienne PONCIN-EPAILLARD<sup>4</sup>,  
Dominique DEBARNOT<sup>4</sup>

<sup>1</sup>Department of Chemistry, Faculty of Science, Al-Azhar University, Cairo, Egypt

<sup>2</sup>Inorganic Chemical Industries and Mineral Resources Division, National Research Centre, Giza, Egypt

<sup>3</sup>Institute of Materials Science and Technology, Technical University Berlin, Berlin, Germany

<sup>4</sup>Institute of Molecules and Materials of Le Mans, CNRS UMR 6283, University of Le Mans, Le Mans, France

Received: 06.08.2018

Accepted/Published Online: 01.11.2018

Final Version: 05.02.2019

**Abstract:** The present study addresses the removal of cadmium ions (Cd(II)) from aqueous solutions at a pH of 7.5 using zeolite-A activated by exposure to oxygen plasma. The activation process was performed over a wide range of plasma powers (10, 20, 30, and 40 W) and exposure times (30 to 360 s). Oxygen plasma cannot chemically modify zeolite to a considerable extent, but it can clean the surface, open blocked pores, and induce the formation of additional OH groups via exposure to humidity in ambient air. Therefore, Cd<sup>+2</sup> ion removal is increased by approximately 10% with the plasma treatments. Infrared-attenuated total reflectance spectroscopy, X-ray diffraction, scanning electron microscopy, and energy dispersive spectroscopy were applied to analyze the changes in the surface structure and properties of the samples.

**Key words:** Cadmium removal, water treatment, zeolite-A, oxygen plasma, zeolite modification

### 1. Introduction

The development of chemical industries has affected the earth over the past several centuries, and some of the effects are negative; for example, water resources have been contaminated by toxic heavy metal residues, such as Pb<sup>+2</sup>, Cu<sup>+2</sup>, Cd<sup>+2</sup>, and Zn<sup>+2,1,2</sup> from different industrial activities.<sup>3</sup> Cadmium (Cd<sup>+2</sup>) is one of the most dangerous elements and is one of the main pollutants in ecosystems, especially in water resources. Cadmium comes from several sources, including mine drainage, battery disposal, and paint production, and is widely distributed globally.<sup>4–6</sup> The harmful effects of heavy metals have been well established in scientific articles, and many diseases, such as anemia, chronic headaches, and diarrhea, have been diagnosed as a result of exposure to low concentrations of these metals.<sup>7</sup> When humans are exposed to high concentrations of toxic metals,<sup>8</sup> the metals can act as powerful neurotoxic agents, leading to irreversible reproductive system damage and hepatic and renal failure.<sup>9</sup>

Several chemical and physical processes have been used to remove toxic metals from water, including coagulation, precipitation, chemical oxidation, ion exchange, membrane separation, electrochemical treatment, and adsorption techniques. Among these methods, adsorption is an effective removal process that is straightforward. Appropriate adsorbents can be found in nature, and therefore, they are easily available and inexpensive.<sup>10,11</sup>

\*Correspondence: alaa.fahmy@azhar.edu.eg

Recently, crystalline microporous materials have continued to have an increasing role in applications to address global issues, such as environmental standards for pollution, the depletion of fossil energy resources, and increasing energy consumption. The interest in such materials is due to their unique properties. Specifically, zeolite materials, which have a crystalline structure with defined pores, have been used in a wide range of applied and fundamental studies and in industrial chemical technology because of their diverse adsorption, catalytic, ion-exchange, and molecular sieve properties.<sup>12</sup> The significance and widespread importance of zeolites are due to their versatile properties and environmentally friendly effects.<sup>13</sup> New technological standards and challenges require constant improvements in microporous materials and discoveries of new, modified materials. For the heavy crude oil demands, microporous compositions with wide and extrawide pores are needed. Therefore, the interest in preparing zeolite-like materials with additional pores is focused on traditional applications and related emerging applications in medical, electronic, and optical fields.<sup>14</sup>

Activation and modification of zeolites by exposure to low-pressure glow discharge plasmas is a promising way to produce zeolites with new special properties. Plasma is an advanced tool that is used to modify material surfaces to improve their adsorption ability. Chemically reactive species are produced by low-pressure glow discharge plasmas, e.g., electronically excited molecules, ions, and free radicals.<sup>15</sup> Water vapor, oxygen, carbon dioxide, bromine, nitrogen, and ammonia are the most commonly used gases for attaching hydroxyl, carbonyl, peroxide, carboxyl, bromide, amino, and/or amide groups onto a substrate's surface.<sup>16–18</sup> Therefore, plasma treatment is a selective tool. Compared to conventional chemical treatment methods, plasma treatments have several advantages: enhanced catalyst activation, lifetime, and selectivity; reduced energy requirements; highly distributed active species; and minimized preparation time. These advantages lead to the various potential applications of plasma-treated materials.<sup>19</sup>

However, previous investigations on plasma treatments of adsorbent materials are limited. For example, Sahin et al.<sup>20</sup> discussed the cold plasma modification process of varied materials, such as Eriochrome Black T (EBT), to improve the adsorption capacity. The maximum adsorption capacities were 6.02–29.41 mg/g for the untreated materials. After the cold plasma treatment of the adsorbents, the removal percentages for EBT increased from 39.96% for the untreated adsorbent to 84.31% after the modification. The term “cold plasma” is used for a low-pressure glow discharge plasma that is characterized by low or moderate gas temperatures.

Oxygen plasma modifies the pore openings in zeolite by physical and chemical effects. The plasma removes organic residues and loosely bonded materials and may enlarge pore openings by sputtering. Moreover, exposure to oxygen plasma can decrease the concentration of  $\text{Na}^+$  ions because of its preferential sputtering, and this was shown with glass fibers by secondary-ion mass spectrometric investigations of the action of low-pressure oxygen plasma.<sup>21</sup> The free positions may be occupied by other ions or  $\text{H}^+$  and form additional interactive OH groups.

Therefore, the aim of the current work was to modify zeolite-A (ZA) surfaces using cold plasma with oxygen as the plasma gas at different plasma power input wattages and times. The structure of ZA is well known and it contains  $-\text{OH}$  groups that act as active sites.  $\text{O}_2$  plasma should be a good indirect source for the formation of additional  $-\text{OH}$  groups; however, additional hydrogen is needed, which can be delivered from adsorbed water in the zeolite.<sup>22</sup> The blocked or half-opened pores can be opened, and the contamination is removed by sputtering. Therefore,  $\text{O}_2$  gas was selected for the modification to increase the concentration of the active sites on the surface of the substrate. Furthermore, the aim of this work was to determine whether the adsorption capacity of ZA for Cd ions decreases or increases after modification.

The quantity of adsorbed cadmium ions was evaluated by microwave plasma atomic emission spectroscopy

(MP-AES). The samples were analyzed using scanning electron microscopy (SEM), infrared-attenuated total reflectance spectroscopy (IR-ATR), and X-ray diffraction (XRD) after the modification and after the adsorption of cadmium ions. This study is one of the first on plasma modification of zeolite for cadmium remediation of synthetic wastewater.

## 2. Results and discussion

### 2.1. Adsorption of cadmium ions

Figure 1a shows the effect of each 60 s of O<sub>2</sub>-plasma treatment using different power inputs on the relationship between the adsorption capacity,  $q_t$ , of untreated and treated zeolite-A (UZA and TZA, respectively) and the contact time with the Cd ion solution.

Clearly, the amount of Cd adsorbed by zeolite-A slightly depends on the power input. Moreover, the Cd uptake was initially lower before reaching the maximum adsorption equilibrium state after approximately 80 min of contact time (Figure 1a).

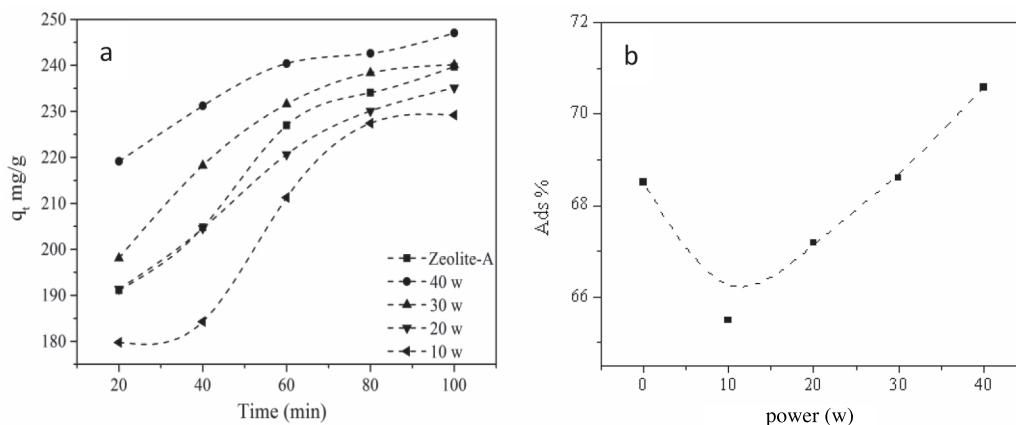
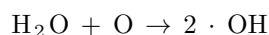
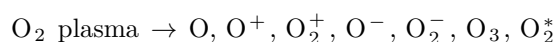


**Figure 1.** (a) Relationship between the contact time and adsorption capacity at various plasma powers; (b) dependence of Cd adsorption on the plasma power used to activate zeolite-A (plasma time = 60 s). The error bars were produced from three different measurements for the same sample.

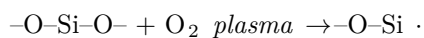
The removal efficiency, i.e. the quantity of cadmium ions adsorbed on the zeolite-A surface, rapidly increased from 68.4% to 71% as the plasma power used to activate the zeolite increased (Figure 1b). A very weak power input was speculated to result in the removal of some hydroxyl groups, and the treatment was not strong enough to generate new sites with –OH groups on the zeolite crystal lattice. A stronger power input produces more defects, which can bond with –OH groups and increase the adsorption capacity.

The results depicted in Figure 1a and Figure 1b can be explained by three observations. First, at a low energy ( $\leq 10$  W), the Cd ion removal efficiency is constant for ca. 20 min, i.e. from 20 to 40 min. Generally, at a low power of 20 W, the adsorption efficiency was lower than that of untreated zeolite-A (UZA<sub>Cd</sub>). The possible reasons for this result were previously discussed. An additional reason may be the zeolite-A particles becoming negatively charged during the oxygen plasma exposure. In the structure of zeolite-A, the SiO<sub>4</sub> tetrahedrons are partially substituted by Al<sup>3+</sup> ions. Thus, the lattice is negatively charged, which can be enhanced by the oxygen plasma treatment. The trapped electrons can form an electron-repulsing surface that affects the adjacent plasma Debye sheath around the particles, hindering further modification of the zeolite structure by electron bombardment from the plasma. Therefore, the sorption capacity of UZA was higher than that of the

TZA with a lower power, i.e. below 20 W, as shown in Figures 1a and 1b.<sup>23</sup> At a power of 40 W, the kinetic energy of the electrons is sufficient to percolate through the negative surface charge of zeolite and to promote the sputtering of sodium ions, formation of hydroxy groups, opening of blocked pores, and removal of (organic) contaminants.<sup>24</sup> Thus, the adsorption rate of modified zeolite-A (TZA<sub>Cd</sub>) increased from 229 to 247 mg/g (removal of cadmium  $\approx$  72%) (Figure 1b). If the wattage is sufficiently high, active species, such as high-energy electrons and reactive radicals, are generated in higher concentrations, resulting in higher concentrations of the active sites and functional groups, such as hydroxyl groups. Additionally, pure thermal activation leads to evaporation of adsorbed water in pores. The oxygen plasma can simply act as an additional cleaner for the surface of thermally activated zeolite, and residual water is required to establish additional hydroxy groups:



These  $\cdot \text{OH}$  species can form the desired  $-\text{OH}$  groups needed for a high Cd adsorption capacity on plasma-activated silicon or aluminum sites.



Cavities and functional groups remain in the inner surface of the zeolite. The plasma is not expected to reach the small pores because of the extraordinary loss of charged species in the walls of the cavities. Nevertheless, microdischarges are reported to form within the catalyst pores of zeolites.<sup>25</sup> The plasma effect being primarily limited to the outer surface may further explain why the Cd adsorption only improved by approximately +10%. Pressure-pulsed plasmas can also modify pores deep in the zeolite by plasma blast waves containing reactive plasma-produced species.<sup>26</sup>

Second, the bond dissociation energies in the structure of zeolite can be summarized as follows: Si–O =  $799.6 \pm 13.4$ , Al–O =  $501.9 \pm 10$ , Na–O =  $270 \pm 4$ , H–O =  $429.91 \pm 0.29$ , and O–O =  $498.36 \pm 0.17$  kJ mol<sup>-1</sup> at 298 K.<sup>27</sup> The lowest bond dissociation energies in the zeolite-A structure are for the Na–O and O–H bonds, which may not contribute to the formation of adhesion-active functional groups, and this explains the low adsorption efficiency values obtained at 20 W, because the Na–O and O–H groups are the main active sites on the surface of zeolite-A. Applying a high plasma energy destroys the active sites (Figure 1b). However, as the plasma power increases, the dissociation of the Si–O and Al–O bonds in the substrate leads to new sources of active sites.

New active centers (Si–OH, Al–OH) can form by the reaction of Si and Al radicals with oxygen species in the plasma and plasma-desorbed residual water molecules in the zeolite or during the postplasma process with water molecules in the air when the zeolite is exposed to air. A high-energy plasma can clearly extensively dissociate the stronger Al–O and Si–O bonds in the zeolite and insert oxygen groups into the surface of zeolite-A.<sup>28</sup> The Al–OH and Si–OH bonds are created by the subsequent hydroxylation reactions of Si or Al radicals that are generated during plasma activation.<sup>29</sup>

Ion exchange is expected to be the main adsorption mechanism of cadmium ions onto zeolite-A, and mainly Na<sup>+</sup> and H<sup>+</sup> ions will be replaced by cadmium ions.<sup>30,31</sup> Na ions are easily sputtered by the plasma, which influences the pH, the newly introduced Si–OH and Al–OH groups, and the Cd adsorption.

Third, the adsorption equilibrium occurred after approximately 80 min, which is when nearly all the active centers on the surface of zeolite-A are blocked by the Cd(II) ions in solution.<sup>32</sup>

Figure 2a shows the effect of different plasma treatment times on the adsorption capacity of O<sub>2</sub>-plasma-exposed zeolite samples as a function of the contact time with the Cd solution. The uptake gradually decreased until a steady-state was achieved after approximately 80 min of contact time. The removal efficiency and quantity of cadmium ions adsorbed on the zeolite-A surface slightly increased from 68.4% to 71% as the plasma exposure time increased to 60 s; longer pretreatment times are disadvantageous (Figure 2b).

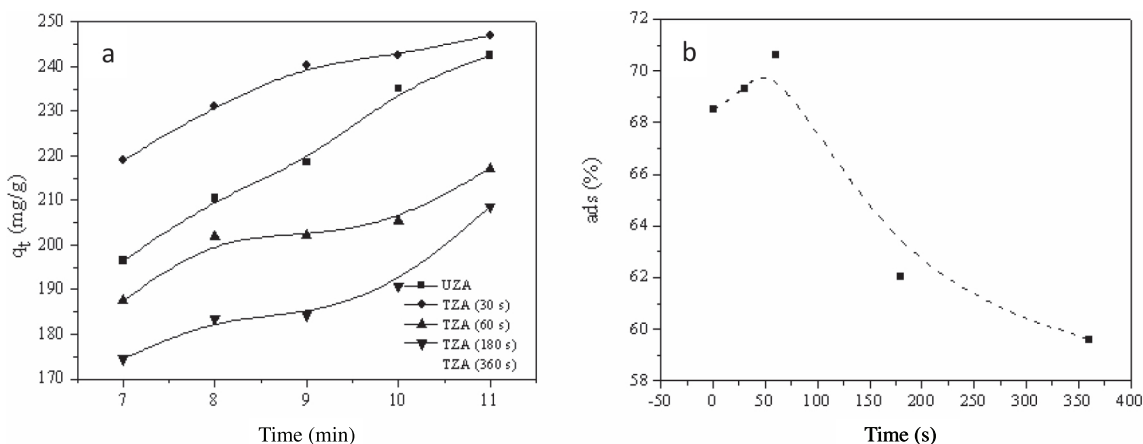


**Figure 2.** The relationship between the contact time and sorption capacity for plasma-modified zeolite samples treated for different plasma times; (b) the adsorption percent versus the plasma time used to activate zeolite-A (power = 40 W).

The results presented in Figures 2a and 2b show the quantities of cadmium ions adsorbed onto the surfaces of TZA and UZA. The oxygen plasma treatment rapidly increased the adsorption capacity of zeolite-A after a 60 s of exposure from 229 to 247 mg/g (cadmium removal  $\approx$  72%), but then the adsorption capacity decreased up to approximately 360 s. However, excessive plasma treatment leads to the destruction of zeolite-A surface functional groups by a condensation reaction:  $2 \text{ Si-OH (2 Al-OH)} \rightarrow \text{Si-O-Si (Al-O-Al)} + \text{H}_2\text{O}$  (Figures 2a and 2b).<sup>33</sup>

An excessive cold plasma treatment time decreases the adsorption capacity. Generally, the zeolite-A adsorption efficiency after 60 s of plasma treatment was higher than that for zeolite-A without pretreatment. If the energy is enough for 60 s, active species, such as high-energy electrons and reactive radicals, are generated during the plasma treatment and can activate the surface of zeolite-A by increasing the number of active sites or/and creating functional groups, such as the previously discussed oxygen groups. However, excessive exposure of zeolite-A to oxygen plasma (360 s) leads to the destruction of surface functional groups on zeolite-A. Similar conclusions were reported by Roland et al., and they detected the formation of stable Al-O-O\* paramagnetic species (lifetime of >14 days).<sup>34</sup> The high plasma power input can also be assumed to degrade the top surface layer of the zeolite structure and create separate Al<sub>2</sub>O<sub>3</sub> and SiO<sub>2</sub> clusters. The granularity of the grains on the catalyst surface was observed to decrease, and the distribution was more uniform after the discharge exposure. These result in the formation of ultrafine particles with a higher specific surface area and a crystal lattice with many vacancies.<sup>35</sup> These physical modifications generate a higher catalytic activity, partially explaining the synergetic effect of plasma catalytic systems. The BET measured surface areas revealed partial baking of the surface, and the area of HZSM-5 (zeolite catalyst) decreased by approximately 45% after the plasma exposure.<sup>36</sup>

As previously mentioned, Na–O ( $\text{Na}^+ \text{O}^-$ ) and O–H ( $\text{O}^- \text{H}^+$ ) have the lowest bond dissociation energies in the zeolite-A structure. Applying a high plasma power destroys the active sites (Figure 2b). However, as the plasma exposure time increases, the bond dissociations of Si–O and Al–O units in the substrate may produce new active sites and thus the plasma exposure time should be limited to 60 s. Furthermore, high energy can dissociate the Si–O and Al–O bonds.

The adsorption–desorption equilibria of the molecules at the surface are greatly influenced by the plasma discharge and the interactions between the adsorbed molecules and the polar surfaces, and the electrostatic forces are more important than the van der Waals forces.<sup>37</sup> This effect can be quantified by the specific interaction parameter of polar solutes.<sup>38</sup> This parameter considers surface properties in terms of potential and acid–base interactions and includes the different interactions (physical or electric) between molecules, such as Keesom and Debye interactions or hydrogen bonding.<sup>39</sup> Moreover, the regeneration of zeolite-A was tested; therefore, zeolite-A blank samples were reused after adsorption of cadmium ions three times and compared to that activated by plasma at power of 40 W. The adsorption efficiency for blanks was 52.16%, 47.63%, and 41.09%, while it was 64.32%, 60.43%, and 53.25% for activated zeolite. These results confirm that the activation process of zeolite-A was performed successfully by plasma radiation. Additionally, the Table reveals the adsorption capacities of cadmium ions that were adsorbed on various kind of zeolites at different conditions, such as the initial concentration of metal ions, amount of zeolite, and pH values. It was observed that the values of adsorption capacities of Cd ions in the case of activated zeolite using plasma discharge in the current work were 154% and 129%, compared to the maximum values showed for zeolite X and zeolite-A, respectively, proving that the cleaning and/or insertion of a new active site occurred on the surface of zeolite-A.

**Table.** Adsorption capacities of cadmium ions adsorbed on different types of zeolites.

Name of zeolite	Adsorption capacity of $\text{Cd}^{+2}$ ions (mg/g)	Experimental conditions	Ref.
Zeolite X	160	Initial metal concentration (20–2000 mg/L), amount of zeolite (2 g/L)	40
Zeolite NaP1	50.0	Initial metal concentration (100 mg/L), pH (3–6), amount of zeolite (2.5–5 g/L)	41
Chabazite	6.70	Initial metal concentration (1–30 mg/L), pH (3–6), amount of zeolite (5 g/L)	42
Zeolite-A	191	Initial metal concentration (1000 mg/L), pH (7.5), amount of zeolite (1–4 g/L)	Present study
Modified zeolite-A	247	Initial metal concentration (1000 mg/L), pH (7.5), amount of zeolite (1–4 g/L)	Present study

## 2.2. XRD

The low-pressure oxygen plasma treatment of ZA did not remarkably affect the intensities and positions of the peaks in the XRD spectra, which indicated that the plasma treatment did not change the basic structure of the ZA samples, agreeing well with the data reported by Oh et al.<sup>43</sup>

Figure 3 shows the XRD patterns for UZA, TZA, UZA with adsorbed cadmium ions ( $\text{UZA}_{\text{Cd}}$ ), and TZA with adsorbed cadmium ions ( $\text{TZA}_{\text{Cd}}$ ). The sharp and strong peaks of the XRD pattern indicated a crystalline

zeolite material that matches Linde type A (LTA) PDF #73-2341 with the formula  $\text{Na}_{12}\text{Al}_{12}\text{Si}_{12}\text{O}_{48}\cdot 27\text{H}_2\text{O}$ , indicating that the plasma treatment did not change the basic structure of the zeolite-A samples discussed before.

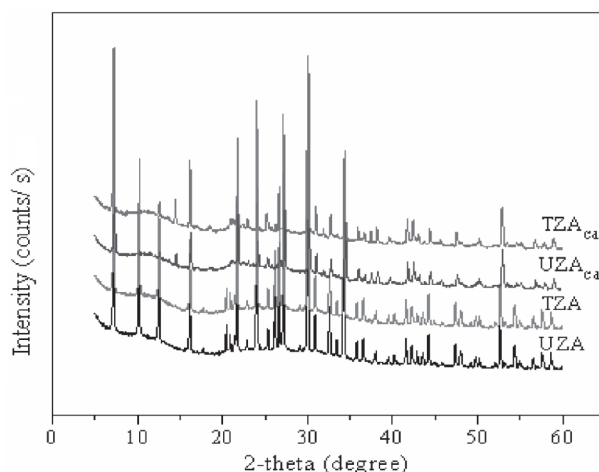


**Figure 3.** XRD patterns of UZA, TZA, UZA<sub>Cd</sub>, and TZA<sub>Cd</sub>.

Notably, the peaks of the cadmium-loaded TZA and UZA decreased, which may be explained by the instability of the zeolite powder in relatively acidic media during the approx. 2 h of cadmium treatment compared to its strongly basic characteristic after its synthesis.<sup>44</sup>

### 2.3. IR-ATR analysis

An IR analysis in the ATR mode was carried out before and after the plasma treatment to identify the main functional groups of zeolite-A that are responsible for the adsorption of cadmium ions. The spectra of the samples were measured in the wavenumber range of 400–4000  $\text{cm}^{-1}$ . The characteristic peaks of zeolite-A at wavenumbers 998  $\text{cm}^{-1}$ , 965  $\text{cm}^{-1}$ , and 671  $\text{cm}^{-1}$  are associated with the Si–O stretching vibration (Figure 4a). The peak at 555  $\text{cm}^{-1}$  is associated with the O–Si–O bonds in the  $\text{SiO}_2$  tetrahedrons. The peak at 461  $\text{cm}^{-1}$  is associated with the Si–O–Si bond.<sup>45</sup>

The IR spectra of zeolite-A before the adsorption process displays several absorption peaks and a broad peak centered at  $\nu \approx 3300\text{ cm}^{-1}$ , which was assigned to the O–H stretching vibration.<sup>46</sup> The peak at  $\nu = 965\text{ cm}^{-1}$  was assigned to the stretching vibration of the Si–O bonds in the  $\text{SiO}_4$  units. The observed absorption band at  $\nu \approx 534\text{ cm}^{-1}$  may be associated with the Si–O–Al stretching vibration with Al in an octahedral coordination environment.<sup>47</sup> The peaks in the range of 1000–900  $\text{cm}^{-1}$  indicated the presence of Si–O, i.e. the crystallization peaks. The peaks in the range of 555–501  $\text{cm}^{-1}$  correspond to the presence of structural double rings of zeolites.<sup>48</sup>

After exposing zeolite-A to  $\text{O}_2$  plasma, the characteristic peaks became sharper and more intense than those of UZA. For example, the intense and broad band at approximately 3660–3070  $\text{cm}^{-1}$  increased after the plasma treatment.<sup>49</sup> This observation is likely due to the morphological changes on the surfaces of the zeolite-A particles. Small contaminants were indicated by peaks at 2930/2880 and 1700  $\text{cm}^{-1}$ , which indicate hydrocarbon structures and carbonyl groups, respectively. The broad peak at 3298  $\text{cm}^{-1}$  decreased in intensity and broadened due to the adsorption of cadmium ions from an aqueous solution, presumably via hydrogen bond formation.

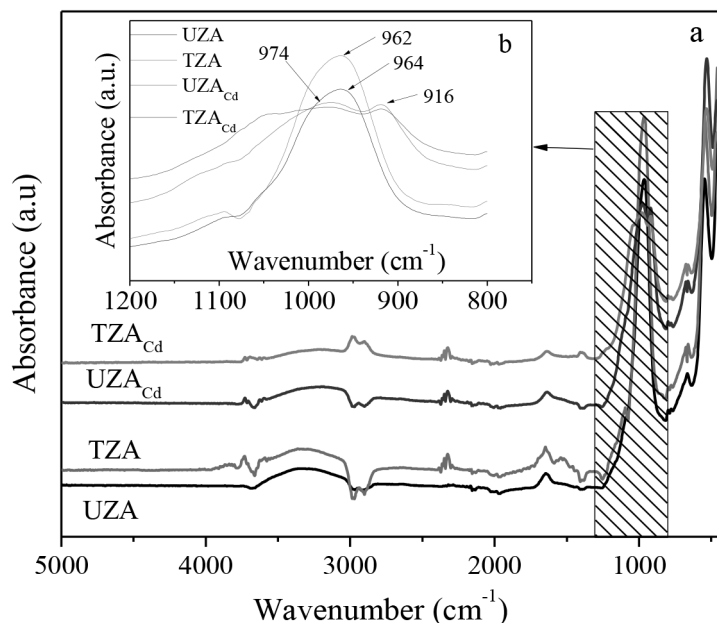


**Figure 4.** (a) IR spectra of UZA, TZA (power = 40 W for 60 s),  $UZA_{Cd}$ , and  $TZA_{Cd}$ ; (b) peak at  $\sim 965\text{ cm}^{-1}$  corresponding to the adsorption of cadmium ions.

Figure 4b reveals that the peak at  $\sim 965\text{ cm}^{-1}$  had a pronounced decrease in intensity due to the adsorption of cadmium ions. The band separated into two peaks, indicating a change in the zeolite structure due to cadmium ion adsorption. These peaks may be related to the bond that forms between the cadmium ions and the active centers on the surface of ZA. Si–O–Cd was observed at  $\sim 916\text{ cm}^{-1}$ , and the second peak for Si–O(–H) appeared at  $974\text{ cm}^{-1}$ .<sup>50</sup> A similar behavior was observed for the TZA sample (Figure 4b). The peak at  $\sim 965\text{ cm}^{-1}$  for TZA was broader than that for UZA, which indicated the long-range order of TZA.

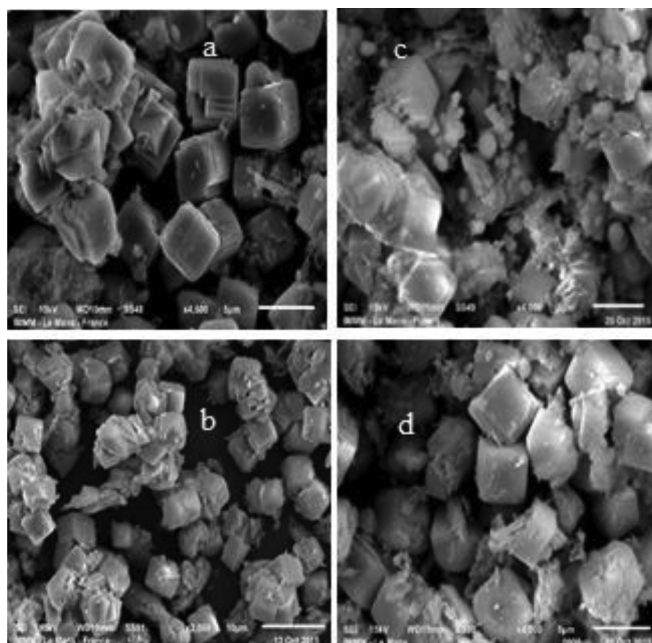
#### 2.4. SEM-EDX analysis

Figure 5 shows the SEM micrographs of the ZA surfaces before and after plasma treatments with different powers (60 s each) and the blank sample for Cd ion adsorption. Well-developed, uniform cubic crystallites characterize the typical morphology of ZA with an average grain size of less than  $5\text{ }\mu\text{m}$ .

The plasma treatment did not have an effect on the cubic structure of the crystallites on the surfaces, as shown in Figures 5a and 5b, which agreed with the XRD data measurements. Figures 5c and 5d depict the effect of the cadmium exchange process on the surfaces of zeolite-A. The crystals slightly decreased in size ( $4\text{--}4.5\text{ }\mu\text{m}$ ), and some undifferentiated structures with rounded edges can be observed. These undifferentiated structures are likely due to the presence of cadmium crystals, which formed because of the ion-exchange process, on the surface of zeolite-A. After adsorption of the cadmium ions, the crystals had a more rounded morphology. The rounded surfaces can be explained by the adsorption of cadmium ions onto the newly developed active sites on the zeolite-A surfaces that were introduced by the plasma exposure. Adsorption via ion exchange inside the pores and on the surface of the adsorbent has been reported to be another possible mechanism.<sup>51</sup>

Figure 6 shows the chemical microanalysis results (EDX) and indicates that the Si/Al elemental ratio is ca. unity, which is the zeolite-A composition ratio given by the XRD stoichiometry of  $\text{Na}_{12}\text{Al}_{12}\text{Si}_{12}\text{O}_{48} \cdot 27\text{H}_2\text{O}$  for the information depth of  $2\text{--}3\text{ }\mu\text{m}$ .<sup>52</sup>





**Figure 5.** (a) SEM images of UZA, (b) TZA - 40 W, (c) UZA after the adsorption of cadmium ions, (d) and TZA - 40 W after Cd ion adsorption.

A significant increase in the oxygen weight percentage, i.e. from 39% to 50%, was observed in TZA compared with that of UZA, which could be related to the formation of new oxygen-containing groups on the surface of ZA as previously discussed. However, the sodium percentages of UZA and TZA (ca. 13%–14%) decreased to 3.6% for  $UZA_{Cd}$  and 1.3% for  $TZA_{Cd}$ , which confirmed the ion-exchange process. Thus, the amount of sodium exchanged for cadmium was approximately 91% for  $TZA_{Cd}$  and 72% for  $UZA_{Cd}$ . However, the amounts of Al and Si (forming the main skeleton of zeolite) also decreased in  $TZA_{Cd}$ , which could be due to the instability of the TZA structure during the cadmium exchange process, as previously mentioned in the XRD results. Similar results were reported in a previous work.<sup>44</sup>

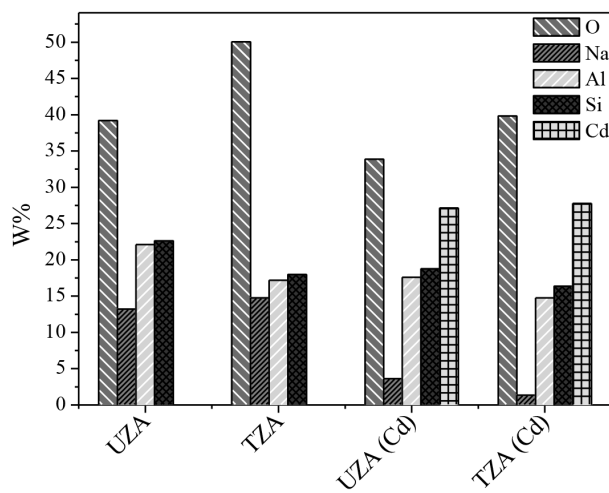


**Figure 6.** Chemical microanalysis (EDX) of treated and untreated zeolite powders, power input = 40 W and time = 60 s.

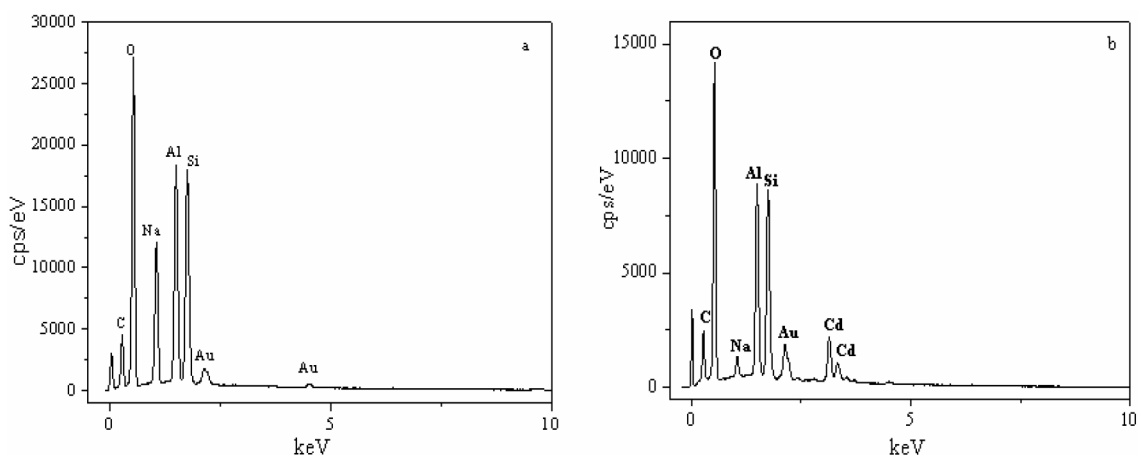


**Figure 7.** (a) Elemental analysis (EDX) of TZA (40 W and 60 s) and (b) subsequent adsorption of cadmium ions.

Al dissolves more readily than Si, which may be the reason for the preferential reduction of Al. The Al content in zeolite is related to the cation exchange capacity (CEC) of zeolite. Most likely, the wastewater cadmium removal mechanism in this case was the CEC of zeolite and surface adsorption onto active sites.

Nevertheless, the Al/Si elemental ratio in TZA<sub>Cd</sub> did not significantly shift. The decrease in both the Al and Si concentrations was caused by the overadsorption of Cd (Figure 7).

## 2.5. Conclusions

Synthetic zeolite-A was prepared from Egyptian kaolin using a microwave technique. The obtained zeolite material was used as a sorbent to remove Cd<sup>2+</sup> ions from wastewater as a model for removing toxic heavy metals from aqueous solutions. Zeolite-A can remove Cd(II) from aqueous solutions with a high efficiency due to its ion-exchange property and hydrophilicity (OH groups). Zeolite-A is a self-supported sorbent and can be applied in a membrane form or as a thin film on different surfaces.

To enhance the adsorption capacity of synthetic zeolite-A, an oxygen plasma treatment was applied. The low-pressure plasma modification of zeolite-A was evaluated with respect to the most significant plasma parameters, i.e. the power input and exposure time. New active sites on the surface of zeolite-A and possibly in the pores were likely generated by the plasma treatment and enhanced the ion-exchange capacity of zeolite-A. The results showed that the removal of metal ions could be improved. The treated zeolite-A adsorption capacity depends on the plasma power input and increased from 229.2 to 247.05 mg/g after 60 s of exposure time as the power increased. Therefore, zeolite-A can be easily prepared from cheap materials and be improved using a simple oxygen plasma treatment. The adsorption capacities of Cd ions by activated zeolite using plasma discharge are higher than the maximum values showed for zeolite-X and zeolite-A by more than 50% and 29 %, respectively, confirming that the insertion of new active site on the surface of zeolite-A happened. This modified material can be used to purify wastewater or utilized as a catalyst.

## 3. Experimental

### 3.1. Plasma treatment

Zeolite-A was prepared by a microwave irradiation process using Egyptian kaolin.<sup>53</sup>

After the preparation, the samples were placed in the discharge chamber, which was composed of stainless steel with dimensions of 30 × 15 × 10 cm (4.5 dm<sup>3</sup>). A flat, rectangular electrode in the upper part of the

chamber was powered by a radio-frequency (rf) generator via a matching network. The rf generator operated at an industrial frequency of 13.56 MHz.<sup>54</sup> The power output varied from 10 to 40 W to ignite the continuous-wave plasma for 0.5 to 6 min. The oxygen flow rate was 10 sccm, and the pressure was  $9.0 \times 10^{-2}$  mbar. To avoid considerable losses of adsorbed water under vacuum, the zeolite was maintained near room temperature during the plasma treatment.

### 3.2. Materials and synthetic wastewater preparation

A stock solution of cadmium ions (chemical compound:  $\text{CdCl}_2$ ; molecular weight: 183.32 g/mol; purity: 99.99%; Sigma-Aldrich) was prepared by dissolving a calculated mass in a known amount of distilled water. In our previous study,<sup>55</sup> zeolite-A was used as an adsorbent for cadmium ions solution at different pH values (6.0, 6.5, 7.0, and 7.5). The removal percentages were 95.15%, 96.86%, 97.5%, and 99.91%, respectively, indicating that the adsorption of cadmium ions is strongly pH-dependent and increases with the pH increase until it reaches a maximum at around pH 7.5. Notably, at  $\text{pH} > 7.8$  cadmium ions formed precipitates and separated by a chemical precipitation process. Therefore, the pH of the current solutions was adjusted to 7.5 by adding 0.1 M  $\text{NH}_4\text{OH}$  or 0.1 M  $\text{CH}_3\text{COOH}$  and was measured using a pH meter. The loading of zeolite with cadmium was performed at a temperature of 298 K, and 0.1 g of zeolite-A was added to 25 mL of a cadmium solution (initial Cd concentration = 1000 ppm). After 100 min, the cadmium ion solution was filtered to remove the loaded zeolite-A.

The amount of adsorbed Cd(II) ions,  $q_t$  ( $\text{mg g}^{-1}$ ) (adsorption capacity), per unit weight at time (t), was evaluated using the mass balance equation (Eq. (1)):<sup>56</sup>

$$q_t = \frac{C_0 - C_t}{M} V, \quad (1)$$

where  $C_0$  is the initial concentration of Cd(II) ( $\text{mg L}^{-1}$ ),  $C_t$  is the concentration at time t ( $\text{mg L}^{-1}$ ), V is the volume of solution (L), and M is the mass (g) of zeolite-A. The error bars result from 3 different measurements of the same sample. Adsorption % (ads %) was defined as in Eq. (2):

$$\text{ads}\% = \frac{C_0 - C_t}{C_0} 100. \quad (2)$$

### 3.3. Characterization methods

To investigate the changes in the chemical species on the surface and their chemical bonding states before and after the  $\text{O}_2$  plasma treatment of zeolite-A, IR-ATR (France, model VERTEX 70V), XRD spectroscopy (XPERT PRO-PAN Analytical), and SEM (Jeol JSM- 6510 LV) were used. Zeolite-A was metallized before and after the plasma treatment with a thin gold layer (JEOL-JFC 1200 FINE COATER) required for the observation and high-resolution SEM images. To determine the concentration of cadmium ions after the adsorption, MP-AES (France, 4100 MP-AES) was utilized.

## References

1. O'Carroll, D.; Sleep, B.; Krol, M.; Boparai, H.; Kocur, C. *Adv. Water Resour.* **2013**, *51*, 104-122.
2. Dong, H. R.; Guan, X. H.; Lo, I. M. C. *Water Res.* **2012**, *46*, 4071-4080.

3. Sari, A.; Tuzen, M. *J. Hazard. Mater.* **2008**, *157*, 448-454.
4. Arancibia-Miranda, N.; Baltazar, S. E.; García, A.; Romero, A. H.; Rubio, M. A.; Altbir, D. *Mater. Res. Bull.* **2014**, *59*, 341-348.
5. Freyria, F. S.; Bonelli, B.; Sethi, R.; Armandi, M.; Belluso, E.; Garrone, E. *J. Phys. Chem. C* **2011**, *115*, 24143-24152.
6. Prado-Cechinel, M. A.; Ulson de Souza, S. A. G. *J. Clean Prod.* **2014**, *65*, 342-349.
7. Qiu, W.; Zheng, Y. *Chem. Eng. J.* **2009**, *145*, 483-488.
8. Arancibia-Miranda, N.; Baltazar, S. E.; García, A.; Munoz-Lira, D.; Sepúlveda, P.; Rubio, M. A.; Altbir, D. *J. Hazard. Mater.* **2016**, *301*, 371-380.
9. Charlet, L.; Chapron, Y.; Faller, P.; Kirsch, R.; Stone, A.; Baveye, P. *Coord. Chem. Rev.* **2012**, *256*, 2147-2163.
10. Nguyen, T. C.; Loganathan, P.; Nguyen, T. V.; Vigneswaran, S.; Kandasamy, J.; Naidu, R. *Chem. Eng. J.* **2015**, *270*, 393-404.
11. Wang, S.; Peng, Y. *Chem. Eng. J.* **2010**, *156*, 11-24.
12. Corma, A. *J. Catal.* **2003**, *216*, 298-312.
13. El-Roz, M.; Lakiss, L.; Vicente, A.; Bozhilov, K. N.; Thibault-Starzyk, F.; Valtchev, V. *Chem. Sci.* **2014**, *5*, 68-80.
14. Corma, A.; Diaz, U.; Arrica, M.; Fernandez, E.; Ortega, I. *Angew. Chem. Int. Ed.* **2009**, *48*, 6247-6250.
15. Fahmy, A.; El-Zomrawy, A.; Saeed, A. M.; Sayed, A. Z.; Ezz El-Arab, M. A.; Shehata, H. A. *Chemosphere* **2018**, *210*, 102-109.
16. Poncin-Epaillard, F.; Vrlnic, T.; Debarnot, D.; Mozetic, M.; Coudreuse, A.; Legeay, G.; El Moualij, B.; Zorzi, W. *J. Funct. Biomater.* **2012**, *3*, 528-543.
17. Fahmy, A.; Debarnot, D.; Friedrich, J. *J. Adhesion Sci. Technol.* **2015**, *29*, 965-998.
18. Fahmy, A.; Friedrich, J.; Poncin-Epaillard, F.; Debarnot, D. *Thin Solid Films* **2016**, *616*, 339-347.
19. Chang-Jun, L.; Gheorghii, P.V.; Ben, W.; Jang, L. *Catalysis Today* **2002**, *72*, 173-184.
20. Sahin, O.; Saka, C.; Kutluay, S. *J. Ind. Eng. Chem.* **2013**, *19*, 1617-1623.
21. Ivanova-Mumeva, V. G.; Andreevskaya, G. D.; Friedrich, J.; Gähde, J. *Acta Polymerica* **1980**, *31*, 752-756.
22. Fahmy, A.; Friedrich, J. *J. Adhesion Sci. Technol.* **2013**, *27*, 324-338.
23. Zou, J. J.; Liu, C. J.; Zhang, Y. P. *Langmuir* **2006**, *22*, 2334-2339.
24. Kim, H. H.; Ogata, A.; Futamura, S. *Appl. Catal. B Environm.* **2008**, *79*, 356-367.
25. Van Durme, J.; Dewulf, J.; Leys, C.; Van Langenhove, H. *Appl. Catal. B Environm.* **2008**, *78*, 324-333.
26. Friedrich, J. F.; Mix, R.; Schulze, R. D.; Meyer-Plath, A.; Joshi, R.; Wettmarshausen, S. *Plasma Proc. Polym.* **2008**, *5*, 407-423.
27. Luo, Y. R. *Comprehensive Handbook of Chemical Bond Energies*; CRC Press: Boca Raton, FL, USA, 2007.
28. Steffen, H. J.; Schmidt, J.; Gonzalez-Elipe, A. *Surf. Interf. Anal.* **2000**, *29*, 386-391.
29. Rinsch, C. L.; Chen, X.; Panchalingam, V.; Eberhart, R. C.; Wang, J. H.; Timmons, R. B. *Langmuir* **1996**, *12*, 2995-3002.
30. Merrikhpour, H.; Jalali, M. *Clean Technol. Environ. Policy* **2013**, *15*, 303-316.
31. Remenarova, L.; Pipiska, M.; Florkova, E.; Hornik, M.; Rozloznic, M. *Clean Technol. Environ. Policy* **2014**, *16*, 1551-1561.
32. Moradi, O. *Chem. Biochem. Eng. Q.* **2011**, *25*, 229-240.
33. Fahmy, A.; Mohamed, T. A.; Friedrich, J. F. *Applied Surface Science* **2018**, *458*, 1006-1017.
34. Roland, U.; Holzer, F.; Kopinke, F. D. *Appl. Catal. B Environ.* **2005**, *58*, 217-226.

35. Guo, Y. F.; Ye, D. Q.; Chen, K. F.; He, J. C.; Chen, W. L. *J. Mol. Catal. A Chem.* **2006**, *245*, 93-100.
36. Wallis, A. E.; Whitehead, J. C.; Zang, K. *Appl. Catal. B Environ.* **2007**, *74*, 111-116.
37. Blin-Simiand, N.; Tardiveau, P.; Risacher, A.; Jorand, F.; Pasquiers, S. *Plasma Process. Plasma Polym.* **2005**, *2*, 256-262.
38. Diaz, E.; Ordonez, S.; Vega, A.; Coca, J. *Micropor. Mesopor. Mater.* **2005**, *83*, 292-300.
39. Miranda, B.; Diaz, E.; Ordonez, S.; Vega, A.; Diez, F.V. *Chemosphere* **2007**, *66*, 1706-1715.
40. Jha, V. K.; Nagae, M.; Matsuda, M.; Miyake, M. *J. Environ. Manage.* **2009**, *90*, 2507-2514.
41. Álvarez-Ayuso, E.; García-Sánchez, A.; Querol, X. *Water Res.* **2003**, *37*, 4855-4862.
42. Ouki, S.; Kavannagh, M. *Waste Manage. Res.* **1997**, *15*, 383-394.
43. Oh, S. M.; Kim, H. H.; Einaga, H.; Ogata, A.; Futamura, A.; Park, D. W. *Thin Solid Films* **2006**, *506-507*, 418-422.
44. Hartman, R. L.; Fogler, H. S. *Langmuir* **2007**, *23*, 5477-5484.
45. Youssef, H. F.; Hegazy, W. H.; Abo-Almaged, H. H. *J. Porous Mater.* **2015**, *22*, 1033-1041.
46. Feng, N.; Guo, X.; Liang, S. *J. Hazard. Mater.* **2009**, *164*, 1286-1292.
47. Liew, Y. M.; Kamarudi, H.; Al Bakr, A. M. M.; Luqman, M.; Nizar, I. K.; Ruzaidi, C. M.; Heah, C. Y. *Constr. Build. Mater.* **2012**, *30*, 794-802.
48. De Pena, Y. P.; Rondón, W. *Am. J. Anal. Chem.* **2013**, *4*, 387-397.
49. Kosslick, H.; Tuan, V. A.; Fricke, R.; Peuker, C.; Pilz, W.; Storek, W. *J. Phys. Chem.* **1993**, *97*, 5678-5684.
50. Launer, P. J.; Arkles, B., Eds. *Silicon Compounds: Silanes and Silicones*; Gelest, Inc.: Morrisville, PA, USA, 2013.
51. Saravanan, A.; Brindha, V.; Krishnan, S. *J. Adv. Bioinf.* **2011**, *2*, 193-196.
52. Frising, T.; Leflaive, P. *Micropor. Mesopor. Mater.* **2008**, *114*, 27-63.
53. Youssef, H. F.; Ibrahim, D. M.; Komarneni, S. *Micropor. Mesopor. Mater.* **2008**, *115*, 527-543.
54. Vrlinic, T.; Mille, C.; Debarnot, D.; Poncin-Epaillard, F. *Vacuum* **2009**, *83*, 792-796.
55. Fahmy, A.; Youssef, H. F.; Elzaref, A. S.; Shehata, H. A.; Wassel, M. A. *International Journal of Science and Research* **2016**, *5*, 1549-1555.
56. Sadeek, S. A.; Negm, N. A.; Hefni, H. H. H.; Abdel Wahab, M. M. *Int. J. Biol. Macr.* **2015**, *81*, 400-409.